Experimental report

16/02/2022

Proposal: 5-21-1154 **Council:** 4/2020

Title: A High-performance Electrolyte forMonolithic Solid-State Sodium Battery with Al3+ Doped Na3Zr2Si2PO12

Research area: Chemistry

This proposal is a new proposal

Main proposer: Jose Antonio ALONSO

Experimental team: Maria Teresa FERNANDEZ DIAZ

Local contacts: Maria Teresa FERNANDEZ DIAZ

Samples: Na3+2xZr2-xAlxSi2.4P0.6O12 (Al-NZSP, x = 0, 0.1, 0.25)

Instrument	Requested days	Allocated days	From	To
D2B	3	3	26/03/2021	29/03/2021

Abstract:

All solid-state sodium batteries (SSSB) are superior in energy density and safety over sodium ion batteries. Due to the employment of solid-state electrolytes (SSE) and sodium metal anodes, short circuits caused by sodium dendrites may be avoided. Na3Zr2Si2PO12 (NZSP)-type materials meet most of the requirements as promising SSEs. The Na conductivity may be enhanced by suitable elemental doping, achieving sufficient ionic conductivity (>10-3 S cm-1) to satisfy the requirements of SSSBs. We designed novel Na3+2xZr2-xAlxSi2.4P0.6O12 (Al-NZSP, x = 0, 0.1, 0.25) electrolytes where the total conductivity was increased to 4.0×10-3 S/cm. We propose a structural study to discriminate changes in the oxygen coordination and thermal displacement factors of mobile Na+ ions upon Al doping in NZSP. Additionally, this NASICON-like structural type undergoes a structural transition in the 200-300ºC range, from monoclinic to rhombohedral, involving an additional reduction of the activation energy for Na motion. Thus we aim to study the crystal structure evolution across the phase transition, to correlate the changes in the framework with the transport properties.

All solid-state sodium batteries (SSSBs) show their superiority in energy density and safety over sodium ion batteries (SIBs)[1]. Due to the employment of solid-state electrolytes (SSEs) and sodium metal anodes, short circuits caused by sodium dendrites may be avoided [2]. As one of the main component in SSSBs, the $Na_3Zr_2Si_2PO_{12}$ (NZSP)-type materials meet most of the requirements as promising SSEs. Compared with other commonly used sodium ion conductors, such as β-Al_2O_3, borate and chalcogenide-based electrolytes, the NZSP shows intermediate densification temperature, wide electrochemical stable windows, high hardness, and high ionic transference number [3]. The Na conductivity may be enhanced by elemental doping, achieving sufficient ionic conductivity ($>10^{-3}$ S cm^{-1}) to satisfy the requirements of SSSBs.

In this experiment we studied novel Al-doped specimens of composition $Na_{3+2x}Zr_{2-x}Al_xSi_{2.4}P_{0.6}O_{12}$ (Al-NZSP, x = 0, 0.1, 0.25). XRD patterns show that all the peaks can be indexed to a monoclinic structure (JCPDS No. 84-1200) with a space group of C2/c. The total conductivity was increased to 4.0×10^{-3} S/cm, and the grain boundary resistance was remarkably reduced by Al-doping. In order to identify the structural changes introduced in Al-NZSP upon Al doping, neutron powder diffraction experiments (NPD) were carried out to discriminate changes in the oxygen coordination and thermal displacement factors of mobile Na^+ ions. High-resolution NPD patterns were collected for $Na_{3.4}Zr_2Si_{2.4}P_{0.6}O_{12}$ and $Na_{3.5}Zr_{1.9}Al_{0.1}Si_{2.4}P_{0.6}O_{12}$ at the high-resolution D2B neutron diffractometer, with the high-flux mode. The samples were contained in vanadium cans. A wavelength of 1.594 Å was selected from a Ge monochromator.

NASICON structures basically consist of a rigid oxide framework providing four cavities per formula where the conducting cations reside. The cavities become larger as the Si content increases, the compounds reaching a maximum of conductivity for s≈2. We used the original model described by Hong [4] to refine the crystal structure. The NPD diagrams were perfectly indexed the monoclinic *C*2/*c* (No 15) symmetry; no impurities or additional reflections that could have indicated a departure from this symmetry were observed either for x=0 or x= 0.1 samples. In this space group, Zr(Al) atoms and the six inequivalent oxygen atoms, O1 to O6 are located at *8f* (x,y,z) sites; Si was distributed at random with P atoms at 4*e* (0,y,1/4) and 8*f* sites, and its occupancy was fixed to the nominal one. According to Ref [3], Na atoms are located at three distinct sites, Na1 at 4*d* (1/4,1/4,/1/2), Na2 at 4*e* and Na3 at 8*f* Wyckoff sites. Fully occupied Na2 sites are usually described for monoclinic NASICONs, as well as underpopulated Na1 and Na3 positions. Large isotropic thermal displacements were observed for Na atoms, particularly for Na1 and Na3. Preliminary trials to refine the anisotropic displacement factors for Na1 and Na3 failed, lead to a non-positive matrix. Na2 atoms could be refined anisotropically, obtaining values close to an isotropic form; hence, they were considered as isotropic parameters. Difference Fourier maps did not show residual scattering density that may indicate alternative positions for Na ions.

Fig. 1a and 1b show the goodness of both neutron fits. Figure 2 shows a simplified view of the crystal structure for $Na_{3.5}Zr_{1.9}Al_{0.1}Si_2PO_{12}$. The NASICON structure can be broken into fundamental groups of two $(Zr,Al)O_6$ octahedra separated by three $(P,Si)O_4$ tetrahedra, with which they share corners. These basic structural units are joined up by additional corner sharing, resulting in a three dimensional framework providing with conduction channels where Na ions are distributed. Na1 is located at each intersection of three conduction channels in a distorted octahedral coordination. Na2 is at the bend of the zig-zag path in a loose polyhedron with 8 neighboring oxygens. Na3 is connecting two adjacent Na1 sites. The pyramidal coordination of Na3 exhibits an open window across which Na^+ ions may diffuse, typically according with a Na3-Na1-Na3 mechanism, which has been proven functional in monoclinic NASICONs.

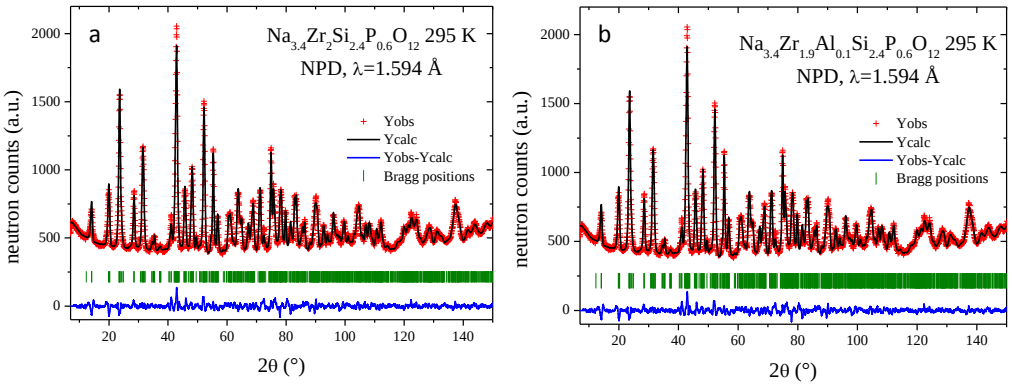

Figure 1: NPD patterns after Rietveld refinements for a) undoped and b) Al-doped phase.

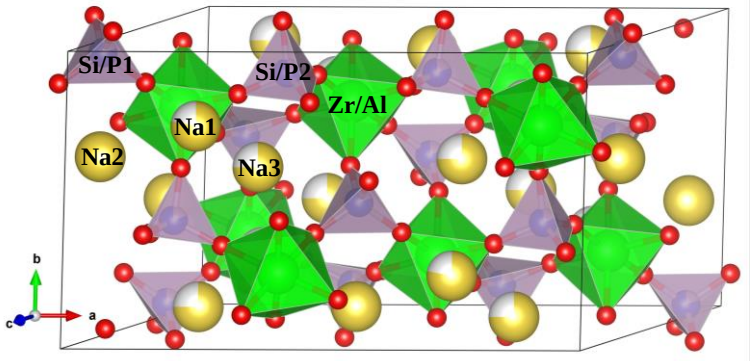

Figure 2: Schematic view of crystal structure of $Na_{3.5}Zr_{1.9}Al_{0.1}Si_{2.4}P_{0.6}O_{12}$.

To unveil the Na^+ pathway in the crystal structure the BVEL maps were calculated. Figure 3 separately illustrates the crystal structure and the BVEL map in two different views, revealing interesting information about the Na^+ diffusion across the crystal structure. It is possible to observe that Na1 cavities have a bigger size and are well connected with Na3 cages, building a plane of strongly connected Na ions within the *b*-*c* plane. This Na1-Na3 connectivity form spirals along the *b*-axis, linked to each other by the sides. In contrast, the

Na2 is weakly connected to Na1, but they allow the connectivity between the planes formed by Na1-Na3. In fact, each Na1 is a connection point between Na2 and Na3, and the mobility of Na^+ in these sites can be ordered in the following sequence Na1>Na3>Na2. These facts explain obtained occupancy factors and the difficulty to refine the anisotropic displacement parameters in these atoms. Additionally, quantitative evidence of the ionic conductivity can be obtained from the percolation energy obtained from $\Delta E_{BVEL}=E_{perc}-E_{min}$. Table 3 lists the ΔE_{BVEL} for each axis and for both compounds. Despite this value cannot be related to the band gap energy obtained from *ab-initio* calculations, a comparison between both Al-doped and undoped phases is enlightening. The ΔE_{BVEL} values also reveal that the mobility in the *b-c* plane is greater than along the *a*-axis. Additionally, the Al-doped phase shows a reduction in the ΔE_{BVEL} in the three axes and an increase in the volume fraction of Na^+ mobility, suggesting an increase in the Na^+ conductivity. The observed reduction in ΔE_{BVEL} vale is 22.8% and 7.14% along the *a*-axis and in the *b-c* plane, respectively, making all three percolations values similar. This result remarkably shows that Al-doped phase approaches to a 3D conductor, as experimentally verified by the transport measurements. This work has been published in Ref. [5].

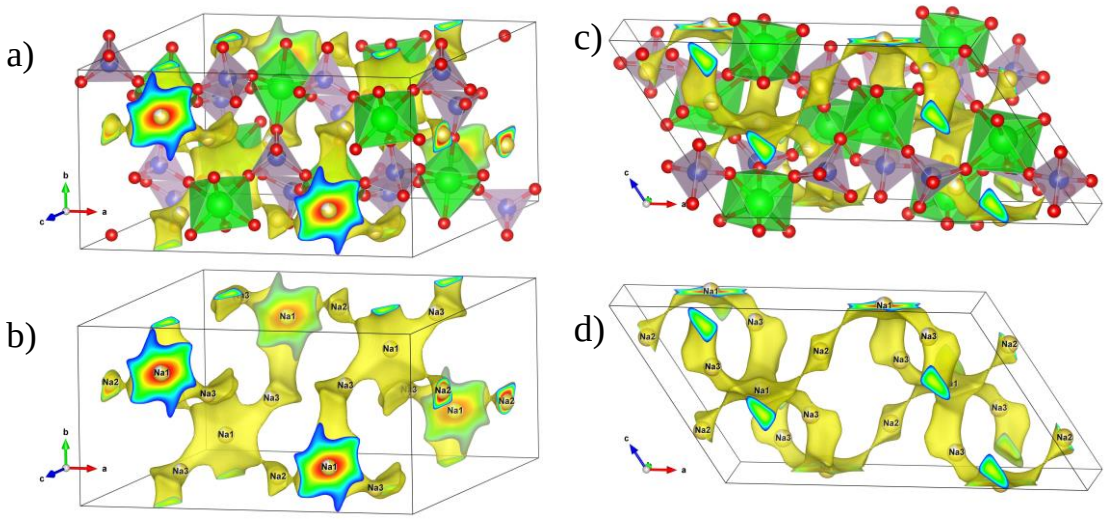

Figure 3: BVEL maps of $Zr_{1.9}Al_{0.1}Si_{2.4}P_{0.6}O_{12}$ phase for ΔE_{BVEL} =1.05 eV, a) and b) along the c-axis and c) and d) along b-axis. a) and c) shows ΔE_{BVEL} over- imposed on the structural skeleton,

References

[1] C. Delmas, *Adv. Energy Mater.* **2018**, *8*, 1703137
[2] C. Zhao, L. Liu, X. Qi, Y. Lu, F. Wu, et al, *Adv. Energy Mater.* **2018**, 1703012.
[3] C. Zhou, S. Bag, V. Thangadurai, *ACS Energy Lett.* **2018**, *3*, 2181
[4] H.Y.P. Hong, Mater. Res. Bull., **1976**, *11*, 173-182.
[5] Lu, Y; Alonso, JA; Lopez, CA; Fernandez-Diaz, MT; Zou, BS; Sun, CW, ACS Appl. Mat. Interfaces **2021**, *13*, 42927-42934.